Lifetimes of low-lying states in ^{125,127}La measured by the recoil distance method

K. Starosta, Ch. Droste, T. Morek, and J. Srebrny
Institute of Experimental Physics, Warsaw University, Hoża 69, PL-00-681 Warsaw, Poland

D. B. Fossan, S. Gundel, J. M. Sears, I. Thorslund, P. Vaska, and M. P. Waring
Department of Physics, State University of New York at Stony Brook, Stony Brook, New York 11794

S. G. Rohoziński and W. Satuła
Institute of Theoretical Physics, Warsaw University, Hoża 69, PL-00-681 Warsaw, Poland

U. Garg, S. Naguleswaran, and J. C. Walpe
University of Notre Dame, Physics Department, Notre Dame, Indiana 46556

(Received 20 January 1997)

Lifetimes of low-lying states in ^{125,127}La nuclei were measured using the recoil distance method. The nuclei were produced by the ^{94}Mo(^{35}Cl,$2p2n$) and ^{112}Cd(^{19}F,$4n$) reactions, respectively. Experimental results were described in the framework of the core quasiparticle coupling model. It was found that the observed bands can be reasonably well described as $\pi g_{7/2}$, $\pi g_{9/2}$, and $\pi h_{11/2}$ quasiparticle configurations coupled to elongated ($\beta_2 \approx 0.28$) triaxial cores. No evidence for a rapid change of the nuclear shape in the $\pi h_{11/2}$ band in ^{127}La is seen in our data. [S0556-2813(97)02506-5]

PACS number(s): 21.10.Tg, 23.20.Lv, 23.20.Js, 27.60.+j

I. INTRODUCTION

It is known that electromagnetic properties of atomic nuclei are sensitive to even tiny details of nuclear wave functions. The empirical data on transition probabilities, branching ratios, etc., in atomic nuclei provide, therefore, valuable information, which improves our knowledge on various aspects of the complex nuclear many-body problem and allows for stringent tests of existing nuclear models. Deviations of nuclear properties from a smooth, systematic behavior are always of particular interest because they may indicate the possibility of new, unexplored phenomena. According to the measurement of Ref. [1], the nucleus ^{127}La shows such unexpected behavior when comparing systematically the reduced matrix elements of electric quadrupole transitions $B(E2;15/2^- \rightarrow 11/2^-)$ in odd-A La nuclei with the $B(E2;2^+ \rightarrow 0^+)$ values in the corresponding even-even Ba and Ce isotones. For example, in ^{129}La, the $B(E2;15/2^- \rightarrow 11/2^-) = 0.42(2)\ e^2\,b^2$ [2] is comparable with the $B(E2,2^+ \rightarrow 0^+)$ values of $0.348(18)\ e^2\,b^2$ and $0.33(2)\ e^2\,b^2$ in ^{130}Ce and ^{128}Ba, respectively [3]. In ^{127}La, the $B(E2;15/2^- \rightarrow 11/2^-)$ value jumps suddenly to $0.87(9)\ e^2\,b^2$ while no increase was found for the $B(E2;2^+ \rightarrow 0^+)$ values in ^{128}Ce and ^{126}Ba, where the $B(E2)$ are $0.43(4)\ e^2\,b^2$ and $0.38(4)\ e^2\,b^2$, respectively [3]. The implied enhancement of collectivity of ^{127}La as compared with its neighbors suggests a significant polarization effect related to the odd proton outside the core. This observed behavior could suggest a substantial change in the nuclear quadrupole deformation either through (i) an increase of nuclear elongation β_2 and/or (ii) a substantial change in the triaxiality γ toward prolate shape.

This unforeseen effect was one of the motivations to study ^{125}La and ^{127}La in greater detail. The present work is complementary to our γ-γ coincidence experiment published in Ref. [4]. While our previous experiment was focused on level structure, here we concentrate on electromagnetic properties of low-lying, one-quasiparticle states. The recoil distance method (RDM) for measuring lifetimes is outlined in Ref. [5]. The low-energy collective states and their electromagnetic properties, such as transition probabilities and branching ratios (combined from the plunger and γ-γ coincidence experiments) are interpreted using the core quasiparticle coupling model (CQPC) [6]. The shape parameters of the cores (CQPC involves both $A+1$ and $A-1$ even-even cores) were deduced from the $E(2_2^+)/E(2_1^+)$ ratios and $B(E2,2_1^+ \rightarrow 0_1^+)$ values in neighboring even-even ^{126}Ba and ^{128}Ce nuclei [3,7]. The deduced cores appear to be triaxial, which is in qualitative agreement with total Routhian surface calculations (TRS's) performed in Ref. [4], where a substantial softness against nonaxial shape distortions was found at low rotational frequencies. The results of the CQPC calculations are in reasonably good agreement with the experimental data. The comparisons do not support any rapid change of the nuclear shape occurring in ^{127}La or ^{125}La.

II. EXPERIMENTAL METHOD AND RESULTS

The lifetime measurements using the recoil distance method [5] were performed at the Stony Brook Nuclear Structure Laboratory using the tandem injected superconducting LINAC facility. An array consisting of five BGO-suppressed Ge detectors in conjunction with the Notre Dame plunger was used. The Ge detectors were placed $\sim$14 cm away from the target at $\pm 30°$, 90°, 125°, and 150° relative to the beam direction. A 14-element BGO multiplicity filter surrounding the target was used to reduce background from Coulex and radioactivity.

The ^{127}La nucleus was populated following the ^{112}Cd (^{19}F,$4n$) reaction at a beam energy of 84.5 MeV. The opti-

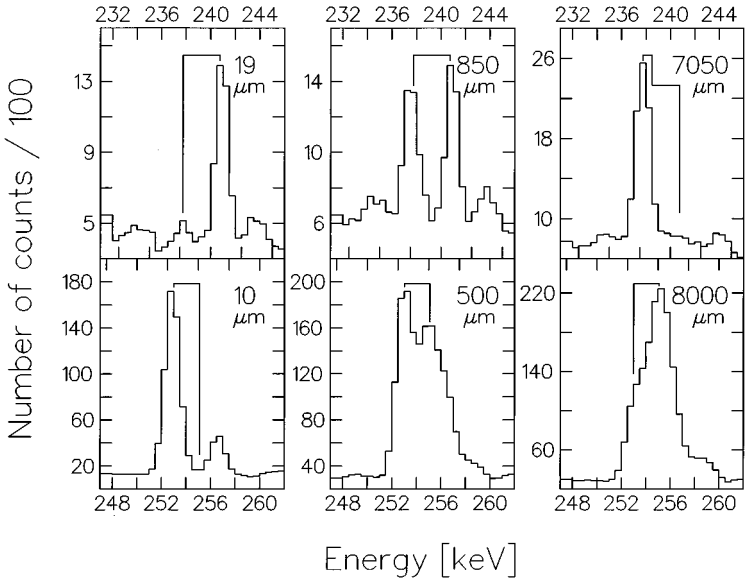

FIG. 1. Examples of the experimental spectra showing shifted and unshifted peaks measured at different target-stopper distances for the 240 keV $15/2^- \rightarrow 11/2^-$ transition in ^{125}La (upper part) and 252 keV $15/2^- \rightarrow 11/2^-$ transition in ^{127}La (lower part). The presented spectra were measured at an angle $\theta = 125°$ for the case of ^{125}La and $\theta = 30°$ for the case of ^{127}La.

mal bombarding energy was determined in our previous study [4]. A 0.58 mg/cm^2 thick target of enriched 98.7% ^{112}Cd was evaporated onto a $\sim$1.3 mg/cm^2 thick gold backing. A gold stopper, $\sim$ 5.0 mg/cm^2 thick, allowed beam particles to pass through but stopped the reaction products. A ^{208}Pb foil $\sim$50 mg/cm^2 thick stopped the beam. The γ-ray spectra were measured for 15 target-stopper distances: 10, 15, 20, 25, 30, 40, 50, 70, 90, 130, 200, 500, 1000, 4000, 8000 μm. The engineering guaranteed the measurement of the relative plunger-stopper separation to be accurate to within $\sim 1\,\mu$m. In addition, the target-stopper distance was controlled by a capacity measurement. The plunger ''zero-point'' position was determined from fits to transitions with short lifetimes ($\tau \leqslant 20$ ps) and was fixed for the rest of data analysis. The average velocity of the ^{127}La recoils was determined to be $\beta = 0.94(4)\%$ from the best linear fit to the $\Delta E_\gamma = E_\gamma \beta \cos\theta$ Doppler-shift relation, where θ is the observation angle and ΔE_γ is the separation between shifted and unshifted peaks corresponding to the γ transition with energy E_γ.

The ^{94}Mo(^{35}Cl,$2p2n$) reaction at a beam energy of 155 MeV was used to populate the excited states of the ^{125}La nucleus. A rolled self-supporting target, 0.55 mg/cm^2 thick, of 94% enriched ^{94}Mo was used together with a $\sim$9.0 mg/cm^2 thick gold stopper to stop the reaction products. The spectra were measured for 16 target stopper positions: 19, 25, 50, 75, 100, 150, 200, 250, 350, 450, 650, 850, 1050, 1650, 3050, 7050 μm. The plunger ''zero point'' and average recoil velocity, $\beta = 2.45(8)\%$, were determined using the same methods as in the case of ^{127}La.

The decay curves for the γ transitions were constructed using two methods of normalization. When the shifted (F) and unshifted (S) peaks were not contaminated, then the ratio of the stopped intensity to the total intensity $R = S/(S+F)$ was formed at each target-stopper distance. When one of the peaks was contaminated then the intensity of the clean peak normalized to the monitor was used to extract the lifetime. To obtain a good statistics, the monitor was constructed as a sum of γ-ray intensities coming from short lived β decays and the total intensities ($S+F$) of strong γ transitions initiated by the reaction and measured at $\theta = 125°$. The decay curves were fitted using the program LIFETIME [8]. The relative intensity of the γ transitions measured at 125° allowed an estimate of the feeding intensity which constrained the fitted parameters. The lifetime of the side feeding was treated as a free parameter in the χ^2 minimization. Figure 1 presents examples of spectra showing shifted and unshifted peaks measured in both experiments. Examples of fitted decay curves are presented in Figs. 2 and 3.

The main corrections considered during the data analysis were due to (a) nuclear deorientation, (b) change in detector solid angles because of the target movement, (c) relativistic effects, and (d) different detector efficiencies for shifted and unshifted peak components.

Nuclear deorientation can lead to gradual changes in angular distributions of γ rays as a function of time [9]. Because of this effect, total intensity ($S+F$) of the γ radiation measured at certain angle θ varies with target-stopper distance. If strong, the deorientation effect may disturb signifi-

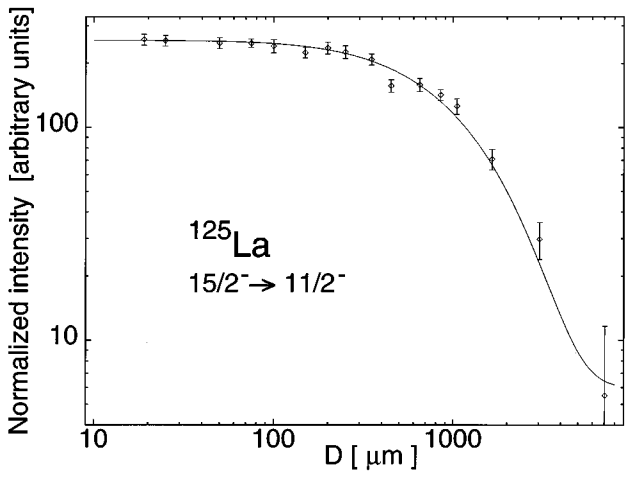

FIG. 2. Decay curve of the 240 keV transition between $15/2^- \rightarrow 11/2^-$ yrast states in ^{125}La measured at $\theta = 125°$.

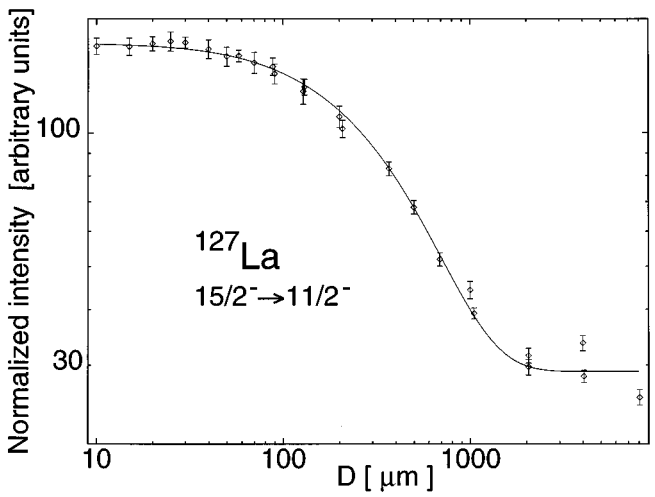

FIG. 3. Decay curve of the 252 keV transition between $15/2^- \rightarrow 11/2^-$ yrast states (states in band 1 in Fig. 4) in ^{127}La measured at $\theta = 30°$.

cantly the decay curve measured with the RDM technique. The second Legendre polynomial $P_2(\cos\theta) \sim 0$ at $\theta = 55°$ and $\theta = 125°$; therefore, lifetimes measured at these angles are considered free from the deorientation effects. In the present experiment, lifetimes measured at different angles were compared. For the $15/2^- \rightarrow 11/2^-$ transition in ^{127}La, the lifetimes measured at $\pm 30°$, 125°, and 150° are equal within error limits. This proves that in case of the ^{127}La experiment the deorientation effects do not play any significant role. This conclusion is confirmed by the agreement between lifetimes of the other transitions measured at 125° and 30° or 150°. For each transition, the results of measurements performed at different angles were averaged to obtained the lifetime, while the difference between these results influenced the experimental error.

The situation is somewhat different in the ^{125}La experiment. Lifetimes of the $15/2^- \rightarrow 11/2^-$ transition measured at $\pm 30°$ and 150° are equal (within the error limit), but $\approx$ 10% shorter than the lifetime measured at 125°. It is believed that this small difference occurs because of deorientation effects, where the recoil velocity is larger than for ^{127}La. The lifetime measured at 125° is taken as the correct value. The lifetimes of the $19/2^-$ level measured at different angles are equal within errors, as is expected for lifetimes shorter than the deorientation time scale.

The solid angle changes calculated for the shifted peaks were smaller than 6% for target-stopper distances between 1 μm and 4000 μm. The γ-ray intensity changes due to the relativistic abberations were on the order of 2% in case of ^{127}La and 4% in case of ^{125}La at $\theta = 30°$. The change of detector efficiency for the shifted and unshifted peaks was found to be smaller than 1% for the ^{127}La experiment and smaller than 1.5% for the ^{125}La experiment. All of these corrections were taken into account in the lifetime evaluation; they were usually comparable with the statistical uncertainties.

The mean lifetimes and transition probabilities evaluated for the excited states in the ^{125}La and ^{127}La nuclei are summarized in Table I. As it is shown below, the values reported in the present paper are consistent with odd-even La systematics. The lifetime of the $15/2^-$ level in ^{127}La disagrees with the result obtained in Ref. [1]. As a byproduct of the present study, the lifetimes of states in ^{128}Ba were extracted; these results are in good agreement with values reported in [10,11] (see Table I).

TABLE I. Results of the recoil distance method mean-lifetime (τ) measurements and transition probabilities derived for excited states in the ^{125}La, ^{127}La nuclei. Energies of γ transitions, spins and parities, band labeling of the ^{125}La, ^{127}La excited states are taken from [4] and Fig. 4. For ^{128}Ba nucleus these data are taken from Ref. [11]. The $B(E2)$ and $B(M1)$ values are based on our results.

Nucleus	E_γ (keV)	Transition I_i	→	I_f	Band	Lifetime (ps)	Previous results (ps)	$B(E2)$ (e^2 b^2)	$B(M1)$ (μ_N^2)
^{125}La	240	$15/2^-$	→	$11/2^-$	1 to 1	145^{+20}_{-35}		$0.65^{+0.20}_{-0.08}$	
	436	$19/2^-$	→	$15/2^-$	1 to 1	$7.7^{+0.6}_{-2.4}$		$0.67^{+0.30}_{-0.05}$	
	604	$23/2^-$	→	$19/2^-$	1 to 1	$\leqslant 3$		$\geqslant 0.34$	
^{127}La	252	$15/2^-$	→	$11/2^-$	1 to 1	140(15)	85(9) [1]	0.53(6)	
	458	$19/2^-$	→	$15/2^-$	1 to 1	$8.0^{+1.5}_{-3.0}$	13.5(1.3) [1]	$0.50^{+0.30}_{-0.08}$	
	631	$23/2^-$	→	$19/2^-$	1 to 1	$\leqslant 4$	$2 \leqslant \tau \leqslant 6$ [1]	$\geqslant 0.20$	
	991	$19/2^+$	→	$19/2^-$	4 to 1	$\leqslant 9.5$			
	177 [b]	$7/2^+$	→	$5/2^+$	2 to 3	140(40)		0.42(16)	0.06(2)
	236 [c]	$7/2^+$	→	$3/2^+$	2 to 2			0.13(4)	
	403	$11/2^+$	→	$7/2^+$	2 to 2	$\leqslant 21$		$\geqslant 0.36$	
^{128}Ba	284	2^+	→	0^+	yrast	140(30) [a]	140(30) [10] 170(12) [11]		
	479	4^+	→	2^+	yrast	36(19) [a]	21(1) [11]		
	644	6^+	→	4^+	yrast	8(3) [a]	13.3(7) [11]		

[a]The effective lifetimes only. No corrections for the deorientation effect and the sidefeeding.
[b]Mixing ratio $\delta = 0.38(5)$ was extracted from the DCO ratio $R_{\mathrm{DCO}} = 0.86(6)$ reported in [4].
[c]$I(177)/I(236) = 6.3(6)$ branching ratio was reported in [4].

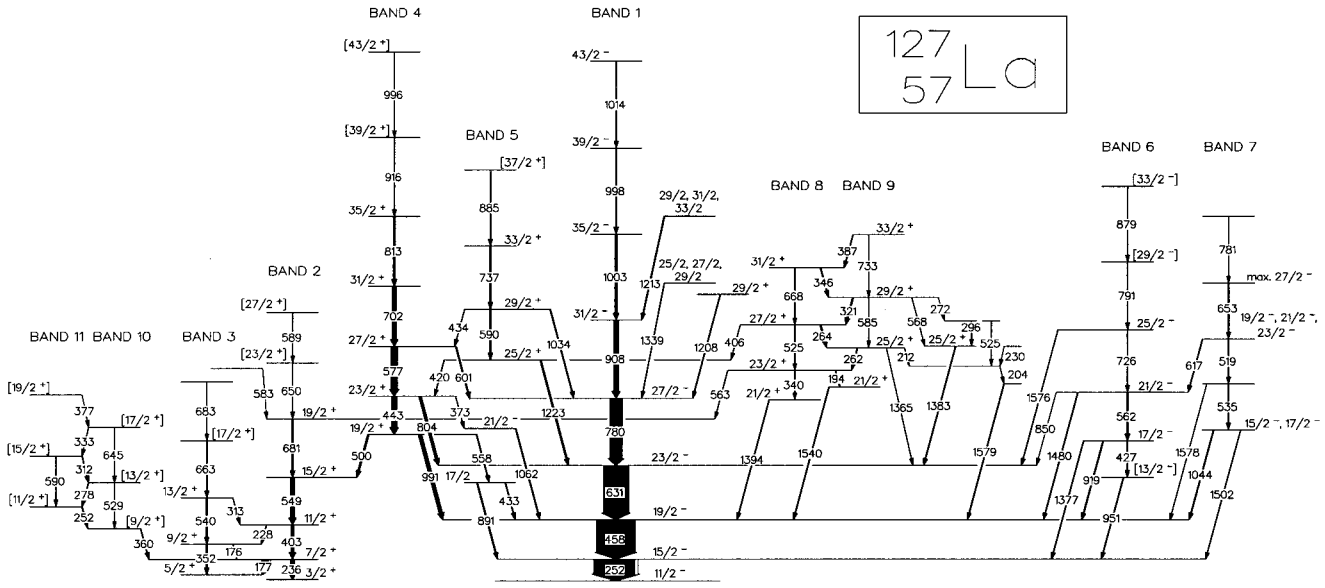

FIG. 4. ^{127}La level scheme proposed in Ref. [4].

III. DISCUSSION OF LOW-LYING STATES IN ^{127}La

A. Core quasiparticle coupling model

The data are interpreted in the framework of the core quasiparticle coupling model (CQPC) developed in Ref. [6], which has been used in previous investigations [12,13]. This model treats an odd-A nucleus as an odd quasiparticle coupled to the neighboring even-even $A-1$ and $A+1$ cores; therefore, its applicability is limited to one quasiparticle states. In the case of $^{127}_{57}$La, the odd proton is coupled to the $^{126}_{56}$Ba and $^{128}_{58}$Ce cores, respectively. The interpretation presented below is limited to ^{127}La since ^{125}La nuclei exhibits similar properties. To facilitate the discussion the level scheme of ^{127}La nuclei proposed in Ref. [4] is shown on Fig. 4. The level scheme of ^{125}La may be found in Ref. [4].

The spectroscopic information for even-even cores (spins, excitation energies, quadrupole matrix elements, etc.), which is needed as input for the CQPC model, was calculated using the triaxial rotor model of Davydov and Filippov [14]. This model was chosen to describe the collective cores because of its simplicity (only three adjustable parameters) and, also, because it reproduces properties of low-lying states in odd-A nuclei almost as reliably as the more sophisticated models, see, e.g., [15]. The three free parameters of the Davydov-Filippov model usually employed, namely the deformation parameters[1] β_0, γ_0, and energy of the first 2_1^+ state $E(2_1^+)$, were adjusted to the experimental data for the ^{126}Ba and ^{128}Ce [3,7] cores separately, see Table II. It is worth noting at this point that the core properties are fixed independently on the odd quasiparticle. The collective core model space, consisting of the 33 lowest states for each core, was used in the calculations. When available, the theoretical excitation energies were replaced by the experimental values to make the calculations more reliable. The single-particle model space of the odd proton was generated by a spherically symmetric Woods-Saxon potential and the states retained in the calculations are shown in Fig. 5. Pairing effects were simulated by a constant gap approximation with $\Delta=135/A$ (MeV). The Fermi level position (see Fig. 5), $\lambda-\varepsilon(d_{5/2})=-0.4$ MeV, was taken to reproduce the number of protons in the La isotopes. The (quasi)particle-core coupling was described by a quadrupole-quadrupole interaction of the same strength as that used before in mass $A\sim130$ calculations[2] of Refs. [15], [16].

The electric-quadrupole, $E2$, and magnetic-dipole, $M1$, single-particle matrix elements were calculated using bare proton charge, $e^{\rm eff}=e$, and standard effective orbital and spin g factors equal to $g_p^{(l)}=1$ and $g_p^{(s)}=0.6g_{\rm free}^{(s)}$, respectively.

TABLE II. Parameters of the even-even cores used in the Davydov-Filippov model.

Core nuclei	β_0	γ_0	$(E2_1^+)$ (keV)
^{126}Ba	0.275	21° (16°) [a]	256
^{128}Ce	0.280	20° (16°) [a]	207

[a] $\gamma_0=16°$ does not follow the experimental data on ^{126}Ba and ^{128}Ce. It is used in part of our calculation concerning the negative parity states, according to the suggestion given in Ref. [21].

B. Positive parity bands

The positive parity bands are treated as collective core states coupled to the quasiparticle states involving $3s_{1/2}$,

[1] The Bohr convention for β and γ parameters is used throughout the paper.

[2] To avoid confusion, it should be noticed that the quoted papers have dealt with only one single-particle orbital and therefore the single-particle radial matrix element was incorporated into the coupling strength. Here we deal with a few single-particle orbitals and use one coupling strength for all of them, multiplying it by the corresponding single-particle radial matrix elements.

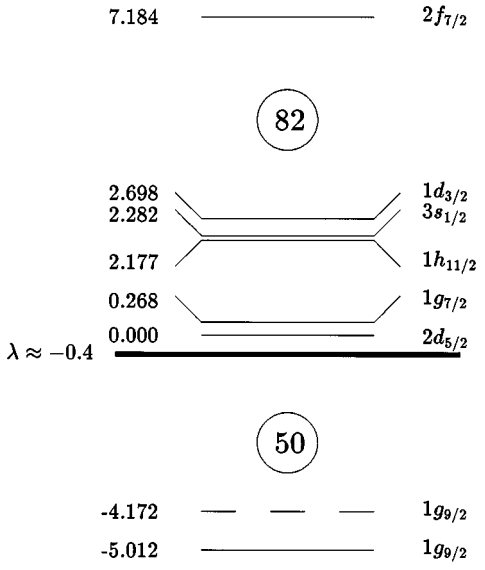

FIG. 5. Single-proton states taken into account in the present calculations. λ denotes the Fermi level position. The broken line is explained in the text. All state energies are given in MeV units.

$2d_{3/2}$, $2d_{5/2}$, $1g_{7/2}$, $1g_{9/2}$ orbitals, see Fig. 5. According to the calculation, the lowest positive parity states, $3/2^+$ and $5/2^+$, have a dominant $d_{5/2}$ component with a small $g_{7/2}$ admixture. Higher members of bands 2 and 3 (see Fig. 6 here and Fig. 4) are essentially the core yrast states coupled to an almost pure $g_{7/2}$ quasiparticle state. This assignment accounts for the ground state spin and gives the proper ordering of the excited levels of bands 2 and 3 as shown in Fig. 6. Note, however, that the excited states of bands 2 and 3 are systematically lower than experimental data by about 200 keV. Although it appeared to be impossible to reproduce absolute excitation energies, the relative excitation energy pattern [except for $\Delta E = E(7/2^+) - E(3/2^+)$] is fairly well reproduced as shown in Table III.

The results for reduced transition probabilities and branching ratios are collected in Table IV. The experimental $B(E2)$ values are systematically larger than the calculated ones. Also, only a qualitative agreement was achieved for

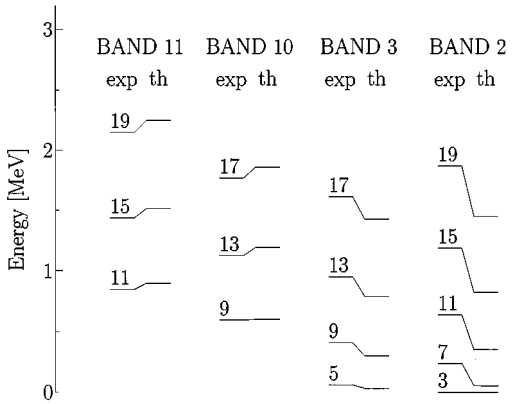

FIG. 6. Low-spin positive parity states in ^{127}La. The experimental data [4] are compared with the results of the theoretical calculations. The band numeration is taken from Fig. 4. The spins are multiplied by the factor 2.

TABLE III. Experimental and theoretical values of the energy difference of states belonging to the bands 2 and 3. All energies are in keV units.

Band	Energy differences			Experiment	Calculation
2	$E(11/2^+)$	-	$E(7/2^+)$	403	300
2	$E(15/2^+)$	-	$E(11/2^+)$	549	471
2	$E(19/2^+)$	-	$E(15/2^+)$	681	628
3	$E(9/2^+)$	-	$E(5/2^+)$	352	269
3	$E(13/2^+)$	-	$E(9/2^+)$	540	492
3	$E(17/2^+)$	-	$E(13/2^+)$	663	641

branching ratios, see Table IV. For bands 2 and 3, the wave functions include a few components with different core states, even if one single-particle state dominates. Such complicated wave functions are sensitive to the model parameters. This may be one of the reasons that the electromagnetic properties, which are very sensitive to the details of the wave function, are not well reproduced. Note that the complexity of the structure of bands 2 and 3 shows up also in the TRS calculations as discussed in Ref. [4] and in the IBFM-2 approach [17].

The best interpretation for bands 10 and 11 involves the $g_{9/2}$ quasiparticle coupled to the successive yrast core states. A similar interpretation was reached in Ref. [4] based on the signature splitting properties of the deformed Nilsson [404]9/2 state extruding from the spherical $g_{9/2}$ subshell. The CQPC model reproduces satisfactorily the relative excitation energies within both bands, see Table V. However, to obtain the correct relative position of bands 10 and 11 with respect to the $3/2^+$ bandhead of band 2, the single-particle $g_{9/2}$ level was shifted up by 840 keV as marked by a broken line in Fig. 5. The interpretation given above is supported additionally by good agreement between the theoretical and the experimental branching ratios as shown in Table VI and moreover by the magnetic moment of the $9/2^+$ state. The magnetic moment for ^{127}La has not been measured yet, but the experimental result for the analogous level [18] in ^{121}Cs is $\mu = 5.4\mu_N$ [19]. The CQPC calculation for both positions of the $g_{9/2}$ orbital gives the value $\mu = 5.1\mu_N$ very

TABLE IV. Experimental and calculated reduced transition probabilities and branching ratios for bands 2 and 3.

Transition			Transition probability Experiment	Calculation
$B(E2,7/2^+$	$\rightarrow$	$3/2^+)$ $(e^2\,b^2)$	0.13(4)	0.05
$B(E2,7/2^+$	$\rightarrow$	$5/2^+)$ $(e^2\,b^2)$	0.42(16)	0.12
$B(M1,7/2^+$	$\rightarrow$	$5/2^+)$ (μ_N^2)	0.06(2)	0.006
Decay			Branching ratio Experiment	Calculation
$7/2^+$	$\rightarrow$	$3/2^+$	100	100
	$\rightarrow$	$5/2^+$	630(60)	190
$11/2^+$	$\rightarrow$	$7/2^+$	100	100
	$\rightarrow$	$9/2^+$	17(1)	6
$13/2^+$	$\rightarrow$	$9/2^+$	100	100
	$\rightarrow$	$11/2^+$	12(3)	2

TABLE V. Energy of levels belonging to bands 10 and 11. The energy of the $9/2^+$ bandhead is assumed to be 0.

Level	Experimental energy (keV)	Calculated energy (keV)
$9/2^+$	0	0
$11/2^+$	252	295
$13/2^+$	529	590
$15/2^+$	841	914
$17/2^+$	1174	1258
$19/2^+$	1551	1645

similar to the experimental one. It supports our interpretation of bands 10 and 11 as the $g_{9/2}$ hole coupled to the collective core.

We also considered a hypothesis where bands 10 and 11 were interpreted as the quasi-γ core band (spin sequence 2_2^+, 3_1^+, 4_2^+, 5_1^+, ...) coupled to either the $d_{5/2}$ or the $g_{7/2}$ quasiparticle state. In these cases the results are much worse, especially for the decay properties. Moreover, the calculated magnetic moments of the $9/2^+$ state in these cases equal $3.4\mu_N$ and $2.6\mu_N$ for the $d_{5/2}$ and the $g_{7/2}$ quasiparticles, respectively, differ significantly from the value of $5.1\mu_N$ discussed above.

As was mentioned above, the lowest $3/2^+$ and $5/2^+$ states have mainly the $d_{5/2}$ configuration. The other states belonging to the $d_{5/2}$ band were not observed in our experiment. Also, the $s_{1/2}$ and the $d_{3/2}$ bands were not observed, which have an excitation energy above 1 MeV, according to our calculations.

C. Negative parity bands

The negative parity bands are treated as collective core states coupled to the negative parity quasiparticle states, $1h_{11/2}$ and $2f_{7/2}$. The interpretation of the yrast band (band 1 on Fig. 4) is quite clear. It is a decoupled band based on the $h_{11/2}$ quasiparticle. Good agreement between theory and experiment concerning both level energies (see Fig. 7) and the intraband reduced transition probabilities (see Table VII) supports this scenario. This interpretation is also reasonably consistent with the results of the TRS calculations of Ref. [4]. Although the TRS calculations predicted the shape of this nuclear state to be prolate, they also indicated a pronounced softness toward triaxial distortions at low rotational frequencies.

The most difficult structure to interpret uniquely is band 6. We performed calculations considering three possible scenarios in which the band originates from different core couplings for the $h_{11/2}$ quasiparticle: (a) the core quasi-γ states 2_2^+, 3_1^+, 4_2^+, 5_1^+, ... forming spin sequence $13/2^-$, $17/2^-$, $21/2^-$, ...; (b) the core quasi-γ states 2_2^+, 3_1^+, 4_2^+, 5_1^+, ... but forming spin sequence $15/2^-$, $19/2^-$, $21/2^-$, ... (these spin values are in disagreement with our assignment for band 6 but were suggested in Ref. [20]); (c) the core yrast states 2_1^+, 4_1^+, 6_1^+, ... and forming a spin sequence as in case (a), i.e., the band is assumed to be signature partner of band 1. Note, that this scenario was not supported by our TRS calculations [4].

TABLE VI. Branching ratios in bands 10 and 11.

Decay			Branching ratio Experiment	Calculation
$13/2^+$	$\rightarrow$	$9/2^+$	100	100
	$\rightarrow$	$11/2^+$	180(20)	227
$15/2^+$	$\rightarrow$	$11/2^+$	100	100
	$\rightarrow$	$13/2^+$	160(30)	138
$17/2^+$	$\rightarrow$	$13/2^+$	100	100
	$\rightarrow$	$15/2^+$	200(80)	99

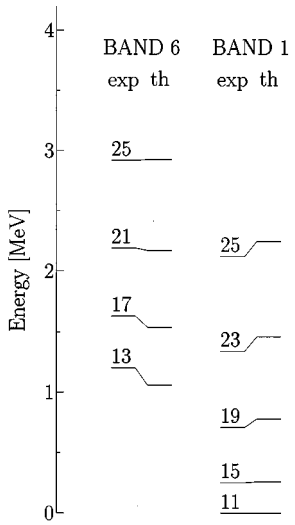

FIG. 7. Low-spin negative parity states in ^{127}La. For band 6 the theoretical data are given according to hypothesis (a). See also caption to Fig. 6.

The comparison of the theoretical spectra and branching ratios with the experimental data gives a preference for hypothesis (a). But even in this case, satisfactory agreement between theory and experiment was achieved only for the level energies, see Fig. 7; the branching ratios are not well reproduced, see Table VIII. Similar difficulties are reported in Ref. [21] for ^{129}La.

The authors of Ref. [21], dealing with the structure of ^{129}La, argue that this nucleus becomes more axial than the neighboring even-even nuclei, because of the $h_{11/2}$ proton driving force. Following that suggestion we performed the calculations for ^{127}La assuming smaller asymmetry parameter, $\gamma_0 = 16°$, for both cores. The value $\gamma_0 = 16°$ is on the border of the limit discussed below. No substantial improvement in the electromagnetic properties for band 6 was achieved and the calculated level energies showed worse agreement.

TABLE VII. Intraband reduced transition probabilities in band 1. All values are given in $(e^2\,b^2)$ units.

Transition			Transition probability Experiment	Calculation
$B(E2;15/2^-$	$\rightarrow$	$11/2^-)$	0.53(6)	0.54
$B(E2;19/2^-$	$\rightarrow$	$15/2^-)$	$0.50^{+0.30}_{-0.08}$	0.59
$B(E2;23/2^-$	$\rightarrow$	$19/2^-)$	>0.20	0.63

TABLE VIII. Branching ratios for the decay of levels from band 6.

Decay			Branching ratio Experiment	Calculation [a]
$13/2^-$	→	$15/2^-$	100	100
	→	$11/2^-$	<10	27
$17/2^-$	→	$19/2^-$	100	100
	→	$15/2^-$	121(17)	44
	→	$13/2^-$	105(14)	3
$21/2^-$	→	$23/2^-$	100	100
	→	$19/2^-$	270(90)	105
	→	$17/2^-$	500(150)	14
$25/2^-$	→	$23/2^-$	100	100
	→	$21/2^-$	100(20)	30

[a]According to hypotheses (a).

It is worth noting, that the γ-decay properties of the $13/2^-$ level in ^{127}La differ from neighboring odd-A lanthanum nuclei [4,21]. In ^{127}La, the $13/2^-$ level decays strongly (with intensity $\geqslant 90\%$) to the $15/2_1^-$ state whereas, for example, in ^{125}La the decay goes with comparable intensities to the $11/2_1^-$ and the $15/2_1^-$ states. This may indicate that the properties of the $13/2^-$ level vary from nucleus to nucleus. It is also possible that in these nuclei, different reactions populate states with different configurations.

A comparison of our experimental data with results of these calculations allows one to estimate, in a model dependent way, the asymmetry parameter γ, see Fig. 8. The value $B(E2,15/2_1^- \rightarrow 11/2_1^-)$ gives an upper limit, $\gamma \leqslant 25°$; a circumspect lower limit, $\gamma > 15°$, is obtained considering the $13/2_\gamma^-$ level energy.

We calculated the $B(E2,\ 15/2_1^- \rightarrow 11/2_1^-)$ values also for odd-A $^{125-131}$La using the same method as applied for ^{127}La. The collective core properties were calculated using the Davydov-Filippov model with parameters β_0, γ_0 and $E(2_1^+)$ obtained from the experimental values of $B(E2,2_1^+ \rightarrow 0_1^+)$, $E(2_2^+)/E(2_1^+)$, and $E(2_1^+)$ in neighboring even-even Ba and Ce nuclei [7,22]. For ^{126}Ce, $\gamma_0 = 19°$ was adopted from systematics. The single-particle subspace was kept fixed for all nuclei but the Fermi level was readjusted accordingly. It is seen from Fig. 9 that the CQPC model well reproduces the experimental $B(E2,15/2_1^- \rightarrow 11/2_1^-)$ values.

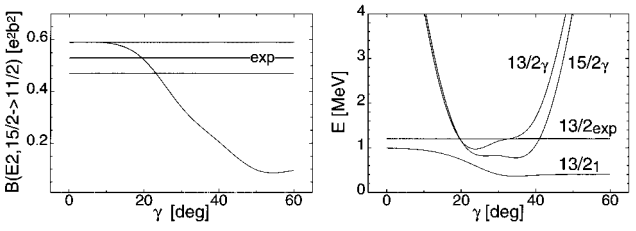

FIG. 8. Reduced transition probabilities $B(E2,15/2_1^- \rightarrow 11/2_1^-)$ and the energies of selected negative parity states as a function of asymmetry parameter γ. It is worth noting that the energies of the $13/2_\gamma^-$ and the $15/2_\gamma^-$ levels increase rapidly when the nuclear shape becomes more axial; this reflects the behavior of the quasi-γ band when the γ parameter tends toward 0° or 60°.

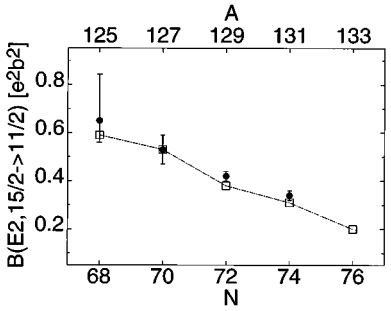

FIG. 9. Comparison between experimental (full circles) and theoretical (open squares) values of $B(E2,15/2_1^- \rightarrow 11/2_1^-)$ for the odd-A lanthanum nuclei with $N = 68-76$. The experimental data were taken for ^{125,127}La from the present paper, for ^{129}La and ^{131}La from [2] and [25].

IV. SUMMARY

The paper summarizes the results of mean lifetime measurements in ^{125,127}La performed using the recoil distance method. The lifetimes, $B(E2)$ and $B(M1)$ values are collected in Table I. The results were analyzed in the framework of the core quasiparticle coupling model using the standard values of model parameters, see Sec. III A for details. The collective core subspace was calculated using the Davydov-Filippov triaxial rigid rotor with inertia parameters deduced from $B(E2,2_1^+ \rightarrow 0_1^+)$, $E(2_2^+)/E(2_1^+)$, and $E(2_1^+)$ values of the even-even $A \pm 1$ neighbors. For ^{127}La this procedure leads to well-deformed ($\beta_2 \approx 0.28$) triaxial cores.

According to the calculations, bands 1,2-3 and 10-11 are interpreted as mainly collective core states coupled to the $\pi h_{11/2}$, $\pi g_{7/2}$, and $\pi g_{9/2}$ quasiparticle states, respectively. Certain difficulties were encountered in the description of the electromagnetic properties of bands 2 and 3. However, band 6 was the most difficult to interpret uniquely. Among different scenarios considered, the most probable configuration seems to involve an $h_{11/2}$ quasiparticle coupled to the quasi-γ core states: 2_2^+, 3_1^+, 4_2^+, 5_1^+, ... Such a configuration was postulated for a similar band in neighboring ^{125}Cs [23]. Our calculations suggest that electromagnetic properties of levels belonging to band 6 could be helpful to distinguish between different hypotheses. Thus, to a unique interpretation one needs more experimental data on the decay properties.

Structures similar to bands 10 and 11 have been observed in this mass region (Sb, I, Cs) and are commonly interpreted as involving a $\pi g_{9/2}$ quasiparticle. Because $\pi g_{9/2}$ extrudes from a shell below the $Z = 50$ gap, these structures have always enhanced β_2 deformation. Moreover, one expects the deformation to increase with Z. Indeed, recently the $\pi g_{9/2}$ band was identified in the $Z = 59$ nucleus ^{131}Pr [24] and its deformation was estimated as $\beta_2 = 0.32$. Our calculations suggest a smaller value of $\beta_2 \approx 0.28$ in $Z = 57$ ^{127}La.

Our measurements do not support the earlier scenario [1] of a rapid change in the deformation of the $h_{11/2}$ band in ^{127}La. The controversial $B(E2)$ value for the $15/2_1^- \rightarrow 11/2_1^-$ transition is estimated as $0.53(6)\ e^2\,b^2$ which nicely follows the systematic trends; a good agreement between theory and experiment was obtained not only for ^{127}La but systematically for odd-A $^{125-131}$La nuclei, see

Fig. 9. Our calculations reveal a gradual increase of β_2 with decreasing neutron number N. In ^{125}La, a deformation as large as $\beta \approx 0.29$ is achieved. Our data do not exclude some changes in nonaxial γ deformation since the calculated $B(E2; 15/2_1^- \rightarrow 11/2_1^-)$ values are rather insensitive to γ deformation for $\gamma_0 \leqslant 20°$ as shown in Fig. 8.

The properties of ^{125}La and ^{127}La are similar. Therefore, the interpretation of bands 1, 2, 3, and 6 in the ^{125}La nucleus (see Figs. 2 and 6 in [4]) is the same as that given above for the ^{127}La nucleus. One should also point out that the interpretation is reasonably consistent with the results of the TRS model [4].

In spite of its simplicity, the CQPC model gives relatively reliable descriptions of low-lying bands for these nuclei. The discrepancies between experiment and theory might be due to, e.g., (i) assumption of rigid triaxial rotor cores in a γ-soft region, and (ii) an oversimplification of the quasiparticle-core interaction.

ACKNOWLEDGMENTS

This work was supported in part by the National Science Foundation (U.S.) and the Polish State Committee for Scientific Research (KBN) under Contract Nos. 2 P302 151 06 and 2 P03B 034 08. The authors would like to thank S. Ćwiok for providing them with Woods-Saxon single-particle spectra, A. Lipski for the preparation of the targets, R. Lefferts and the accelerator crew at the Stony Brook Nuclear Structure Laboratory for providing the beams, and D. C. Radford for providing the RADWARE software package which was used in the data analysis.

[1] P. J. Smith, D. J. Unwin, A. Kirwan, D. J. G. Love, A. H. Nelson, P. J. Nolan, D. M. Todd, and P. J.Twin, J. Phys. G **11**, 1271 (1985).
[2] P. A. Butler, J. Meyer-ter-Vehn, D. Ward, H. Bertschat, P. Colombani, R. M. Diamond, and F. S. Stephens, Phys. Lett. **56B**, 453 (1975).
[3] S. Raman, C. H. Malarkey, W. T. Milner, C. W. Nestor, and P. H. Stelson, At. Data Nucl. Data Tables **36**, 1 (1987).
[4] K. Starosta, Ch. Droste, T. Morek, J. Srebrny, D. B. Fossan, D. R. LaFosse, H. Schnare, I. Thorslund, P. Vaska, M. P. Waring, W. Satuła, S. G. Rohoziński, R. Wyss, I. M. Hibbert, R. Wadsworth, K. Hauschild, C. W. Beausang, S. A. Forbes, P. J. Nolan, and E. S. Paul, Phys. Rev. C **53**, 137 (1996).
[5] D. B. Fossan and E. K. Warburton, in *Nuclear Spectroscopy and Reactions*, edited by J. Cerny (Academic Press, New York, 1974), Part C, p. 341.
[6] F Dönau and U. Hagemann, Z. Phys. A **293**, 31 (1979).
[7] J. Yan, O. Vogel, P. von Brentano, and A. Gelberg, Phys. Rev. C **48**, 1046 (1993).
[8] J. C. Wells, M. P. Fewell, and N. R. Johnson, Report ORNL/TM9105, 1985.
[9] R. Brenn, H. Spehl, A. Weckherlin, H. A. Doubt, and G. van Middelkoop, Z. Phys. A **281**, 219 (1977).
[10] W. Kutschera, W. Dehnhardt, O. C. Kistner, P. Kump, B. Povh, and H. J. Sann, Phys. Rev. C **5**, 1658 (1972).
[11] P. Petkov, S. Harissopulos, A. Dewald, M. Stolzenwald, G. Böhm, P. Sala, K. Schiffer, A. Gelberg, K. O. Zell, P. von Brentano, and W. Andrejtscheff, Nucl. Phys. **A543**, 589 (1992).
[12] M. Brewczyk, S. G. Rohoziński, and W. Urban, Nuclear Physics Laboratory, Annual Report, Warsaw, 1982, p. 36.
[13] Ch. Droste, T. Morek, S. G. Rohoziński, D. Alber, H. Grawe, and D. Chlebowska, J. Phys. G **18**, 1763 (1992).
[14] A. S. Davydov and G. F. Filippov, Nucl. Phys. **8**, 237 (1958).
[15] D. Chlebowska, Ch. Droste, and T. Rząca, Z. Phys. A **303**, 123 (1981).
[16] Ch. Droste, D. Chlebowska, J. Dobaczewski, F. Dönau, A. Kerek, G. Leander, J. Srebrny, and W. Waluś, Nucl. Phys. **A341**, 98 (1980).
[17] J. Genevey, A. Gizon, D. Barneoud, Gh. Căta-Danil, R. Béraud, A. Ensallem, C. Foin, C. F. Liang, P. Paris, and S. Viteritti, Z. Phys. A **356**, 7 (1996).
[18] F. Lidén, B. Cederwall, P. Ahonen, D. W. Banes, B. Fant, J. Gascon, L. Hildingsson, A. Johnson, S. Juutinen, A. Kirwan, D. J. G. Love, S. Mitarai, J. Mukai, A. H. Nelson, J. Nyberg, J. Simpson, and R. Wyss, Nucl. Phys. **A550**, 365 (1992).
[19] S. Raghavan, At. Data Nucl. Data Tables **42**, 189 (1989).
[20] D. Ward, V. P. Janzen, H. R. Andrews, S. M. Mullins, D. C. Radford, and J. C. Waddington, Report TASCC-P-93-3; *Proceedings of the International Conference on Nuclear Physics in Our Times*, Sanibel, Florida, 1992, edited by A.V. Ramayya (World Scientific, Singapore, 1993), p. 218.
[21] R. Kuhn, I. Wiedenhöver, O. Vogel, L. Esser, M. Wilhelm, A. Gelberg, and P. von Brentano, Nucl. Phys. **A594**, 87 (1995).
[22] R. Moscrop, M. Campbell, W. Gelletly, L. Goeting, C. J. Lister, B. J. Varley, and H. G. Price, Nucl. Phys. **A481**, 559 (1988).
[23] J. R. Hughes, D. B. Fossan, D. R. LaFosse, Y. Liang, P. Vaska, and M. P. Waring, Phys. Rev. C **44**, 2390 (1991).
[24] A. Galindo-Uribarri, D. Ward, T. Drake, G. Hackman, V. P. Janzen, S. M. Mullins, S. Pilotte, D. C. Radford, I. Ragnarsson, N. C. Schmeing, and J. C. Waddington, Phys. Rev. C **50**, 2655 (1994).
[25] N. V. Zamfir, A. Dewald, K. O. Zell, and P. von Brentano, Z. Phys. A **344**, 21 (1992).